POLITECNICO DI TORINO
Repository ISTITUZIONALE

Statistical estimation of fatigue design curves from datasets involving failures from defects

(Article begins on next page)

11 February 2024

Statistical estimation of fatigue design curves from datasets involving failures from defects

A. Tridello [a,*], C. Boursier Niutta [a], M. Rossetto [a], F. Berto [b], D.S. Paolino [a]

[a] *Department of Mechanical and Aerospace Engineering, Politecnico di Torino, 10129 Turin, Italy*
[b] *Department of Chemical Engineering, Materials and Environment, Università La Sapienza, 00185, Roma, Italy*

A R T I C L E   I N F O

A B S T R A C T

In the present paper, two methodologies for the estimation of the design curves of datasets with failures originating from defects are proposed. With the first methodology, the Likelihood Ratio Confidence Bound of a specific quantile P-S-N curve is considered. The second method is based on the bootstrap approach, with a large number of datasets simulated starting from the stress life and the defect size distributions estimated from the experimental data. The two approaches have been validated on literature datasets covering also the Very High Cycle Fatigue (VHCF) life region, proving their effectiveness.

1. Introduction

The design of components against fatigue failures is generally carried out with a safe life approach, i.e., the allowable stress that must be considered to withstand the applied loads for the required number of cycles is assessed starting from the stress life relationship (S-N curves) estimated from experimental tests carried out according to International Standards [1,2]. Due to the stochastic nature of the fatigue phenomenon, which is affected by many factors [3–6] like microstructure, type of loads, surface conditions, and manufacturing defects, statistical methodologies [7–12] are employed to model and account for the experimental variability and the related uncertainty in the estimation process, mainly related to the sample numerosity [4]. The Lognormal [9,13,14] or the Weibull distributions [13,15–17] are commonly assumed for the fatigue life distribution and to estimate the Probabilistic-S-N curves (P-S-N curves in the following), with high-reliability quantiles considered for the design of components. However, depending on the specific application, the industrial needs and safety requirements [4], different approaches are employed to estimate the fatigue design curves, i.e., the P-S-N curves to be used for the design of components [4,10,18]. The basic idea is to account also for the uncertainty associated with the estimation process, i.e., rather than considering a deterministic P-S-N curve quantile, the range of uncertainty around it is considered. This uncertainty range tends to increase for datasets with limited amount of data, which is a quite common condition for fatigue data. The design curve generally

corresponds to the lower one-sided confidence interval, computed at a confidence level generally equal to 90%, of a quantile P-S-N curve with a high-reliability level, generally above 90% [4,10]. The estimation of design curves ensuring a safe margin also for datasets characterized by large variability is therefore fundamental for the design of components and of utmost interest among the scientific and industrial community.

Depending on the manufacturing process or on the investigated life range, the origin of the fatigue failure and the site where the crack forms and starts propagating can be different and can affect the variability of fatigue data in the S-N plot. For example, the fatigue response of components produced through Additive Manufacturing (AM) processes is mainly controlled by manufacturing defects, like lack of fusion defects or pores, which lower the fatigue response [19–21], if compared to that of components produced with conventional manufacturing processes. Similarly, defects or impurities are responsible for the crack formation in failures occurring in the Very High Cycle Fatigue (VHCF) life range, but with peculiar mechanisms and with the formation of the so-called Fine Granular Area (FGA), around the initial defect. Datasets covering the Low Cycle Fatigue (LCF)-VHCF life range show a so-called duplex trend on the S-N plot [22,23], with two failure modes, surface and internal failure modes, depending on the life range. The distribution of the defect size within the loaded volume strongly affects the fatigue response, with datasets characterized by large variability in the S-N plot. For these datasets, the safe life approach must be combined with the damage-tolerant approach to properly account for the influence of defects and their size on the fatigue response. In the literature, several models have

Nomenclature

$\sqrt{a_{d,0}}$	square root of the area of the defect, $a_{d,0}$.
α	reliability level.
C	confidence.
cdf	cumulative distribution function.
c_Y, m_Y, n_Y	constant coefficients of the statistical distribution of the fatigue life.
c_{sl}, c_{th} and α_{th}	constant coefficients of the statistical distribution of the fatigue limit
$c_{\sqrt{A_{FGA}}}, m_{\sqrt{A_{FGA}}}$ and $n_{\sqrt{A_{FGA}}}, \sigma_{\sqrt{A_{FGA}}}$	parameter of the FGA statistical distribution.
$c_{Y,surf}, m_{Y,surf}, \sigma_{Y,surf}$	parameters of the cdf of the fatigue life for surface failures.
DMLS	Direct Metal Laser Sintering.
$F_{X_l\|\sqrt{a_{d,0}}}(x; \sqrt{a_{d,0}})$	cdf of the logarithm of the fatigue limit random variable, $X_l\|\sqrt{a_{d,0}}$
$F_{Y\|\sqrt{a_{d,0}}}(y; x, \sqrt{a_{d,0}})$	cdf of the conditional fatigue life.
$F_{\sqrt{A_{FGA}}}$	cumulative distribution function of the Fine Granular Area random variable $\sqrt{A_{FGA}}$
$F_Y(y; x)$	cdf of the marginal fatigue life.
$F_{Y\|surf}(y; x), F_{Y\|int}(y; x), F_{X_t}(x)$	cdf of the fatigue life for surface, internal failures and of the transition stress.
$f_{Y\|X=x}$	probability density function (pdf) of the fatigue life distribution.
$f_{\sqrt{A_{d,0}}}(\sqrt{a_{d,0}})$	pdf of the LEVD.
θ	parameter to be estimated.
$\widetilde{\theta}$	best fitting parameters.
$L[\theta]$	Likelihood function.
LEVD	Largest Extreme Value Distribution
LRCB	Likelihood Ratio Confidence Bound.
n_d	number of simulated datasets
μ_{X_t}, σ_{X_t}	mean and standard deviation of the cdf of the transition stress.
$\mu_Y(\bullet)$	mean of the statistical distribution of the fatigue life
μ_{X_l}	mean of the cdf of the fatigue limit
pdf	probability density function.
$PL[s_{a,\alpha}]$	Profile Likelihood function.
R	reliability.
SIF	Stress Intensity Factor
$s_{a,\alpha}$	α-th quantile of the fatigue strength at the investigated number of cycles to failure.
σ_Y, σ_{X_l}	standard deviation of the fatigue life and fatigue limit
x	logarithm of s_a (applied stress amplitude).
y^*	logarithm of the runout number of cycles.
y	logarithm of n_f (number of cycles to failure).
$\chi^2(1; 1-\beta_{th})$	$(1-\beta_{th})$-th quantile of a Chi-square distribution with 1 degree of freedom.

been proposed to model the influence of defects on the fatigue life [5,24–28] or to model the P-S-N curve of datasets covering the Low Cycle Fatigue (LCF) – VHCF life range with the duplex trend [10], but none of these focus on methodologies for the estimation of the design curves, to the Authors' best knowledge.

In the present paper, two methodologies for the estimation of the design curves of datasets with failures originating from defects are developed. The first methodology is based on the Maximum Likelihood Principle, with the design curve estimated as the lower Likelihood Ratio Confidence Bound of a high-reliability quantile P-S-N curve. The second method is based on the bootstrap approach, with a large number of datasets simulated starting from the stress life distribution estimated from the experimental data. Random defects are also simulated to model their influence on the fatigue response and, for failures originating in the VHCF region with FGA formation, the dependence between the defect size and the FGA size is also accounted for. The two approaches have been validated on several datasets that can be best-fitted with models describing a linear trend, a linear trend with fatigue limit and a duplex trend, proving their effectiveness and their potentialities.

2. Design curve in presence of defects: Likelihood ratio confidence bound

This section focuses on the methodologies for estimating the design P-S-N curves from datasets with failures originating from defects. In the following, the design curve is assumed as the $R(1-\alpha)\%C\alpha_C\%$ S-N curve, according to the notation in [4,10,18]. Accordingly, the design curve is the lower bound, at the $\alpha_C\%$ confidence level, of the $\alpha\%$ quantile P-S-N curve (Reliability level $(1-\alpha)\%$). For example, the R95C90 design curve corresponds to the S-N curve obtained by estimating the 90% lower confidence bound (confidence C equal to 90%) of the 0.05-th quantile P-S-N curves (i.e., reliability R equal to 95%). Accordingly, the uncertainty associated with the α-th quantile P-S-N curve is also accounted for, increasing the safety margin with respect to failures, fundamental for datasets characterized by large variability and limited numerousness. Indeed, the scatter of the experimental data in the S-N plot tends to

increase when fatigue failures originate from defects, due to their size variability and their random location within the loaded volume of parts subjected to non-uniform stress distributions [5,29,30].

Several models have been proposed by the Authors to assess the stress-life relationship of datasets with failures from defects. However, the issue concerning the estimation of the design P-S-N curves for datasets with defects at the origin of the fatigue failures has never been addressed and is the objective of the present work.

Two methodologies will be exploited for the estimation of the design curve: this section focuses on the first methodology, based on the Likelihood Ratio Confidence Bound (LRCB). In Section 2.1, the general procedure developed for the estimation of the design curve with the LRCB is described. Sections from 2.1.1 to 2.1.4 provide details for the application of the proposed methodology to models proposed by the Authors in the literature (i.e., conditional and marginal linear models, marginal model with linear trend and fatigue limit and duplex model) [9,24,31–33].

In the following, the characteristic defect size is assumed as the square root of the area of the defect projected in a direction perpendicular to the maximum applied stress according to [5].

2.1. Likelihood ratio confidence bound: Methodology

The design curve as the lower LRCB of a specific quantile of the P-S-N curve is assessed starting from the estimation of the unknown material parameters of the considered fatigue life distribution. The parameter estimation is carried out by applying the Maximum Likelihood Principle, i.e., by maximizing the Likelihood function, $L[\theta]$, reported in Eq. (1):

$$L[\theta] = \prod_{i_f=1}^{n} f_{Y\|X=x}[y_{i_f}; x_{i_f}; \theta] \bullet \prod_{j=1}^{n_r}(1 - F_{Y\|X=x}[y^*; x_j; \theta]) \tag{1}$$

being θ the set of unknown parameters to be estimated, $f_{Y\|X=x}$ the probability density function (pdf) of the fatigue life distribution, y^* the logarithm of the runout number of cycles, y and x the logarithm of n_f (number of cycles to failure) and s_a (applied stress amplitude), respectively. The subscript i_f ($i_f = 1\cdots n$) refers to failure i_f, whereas the
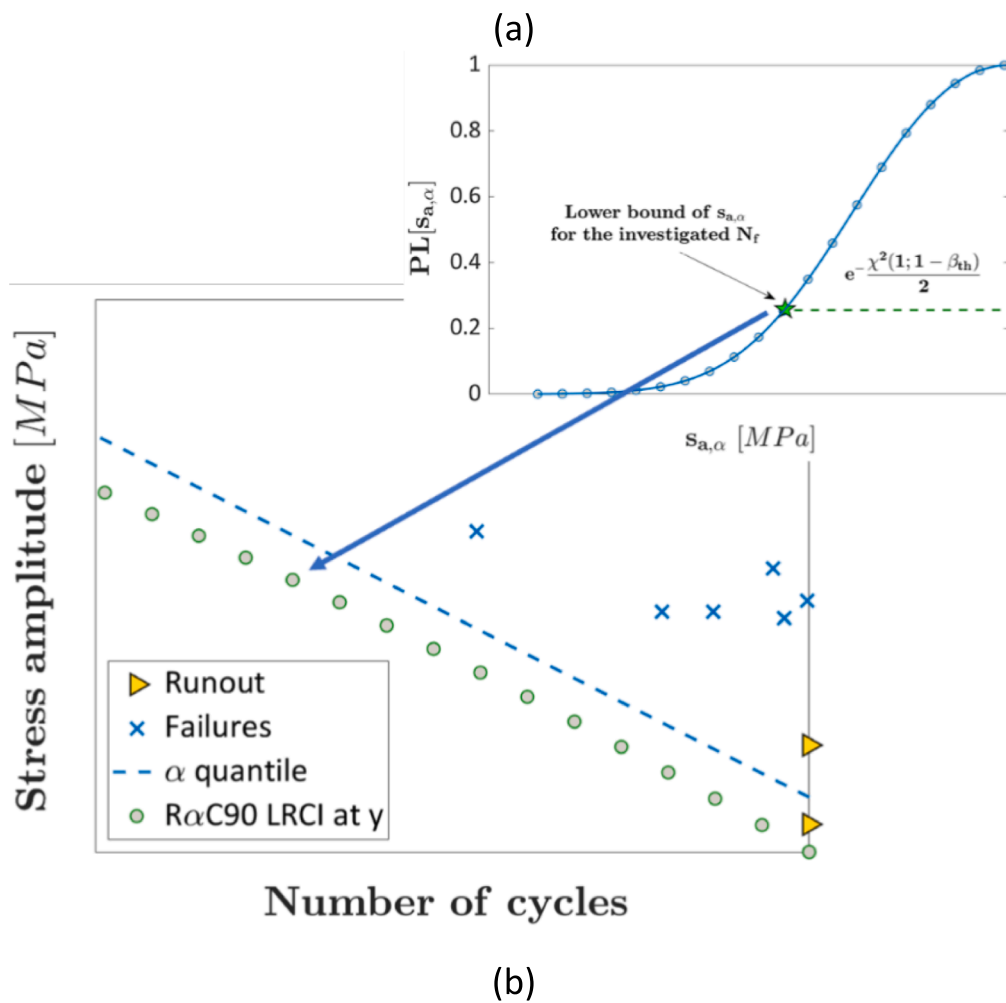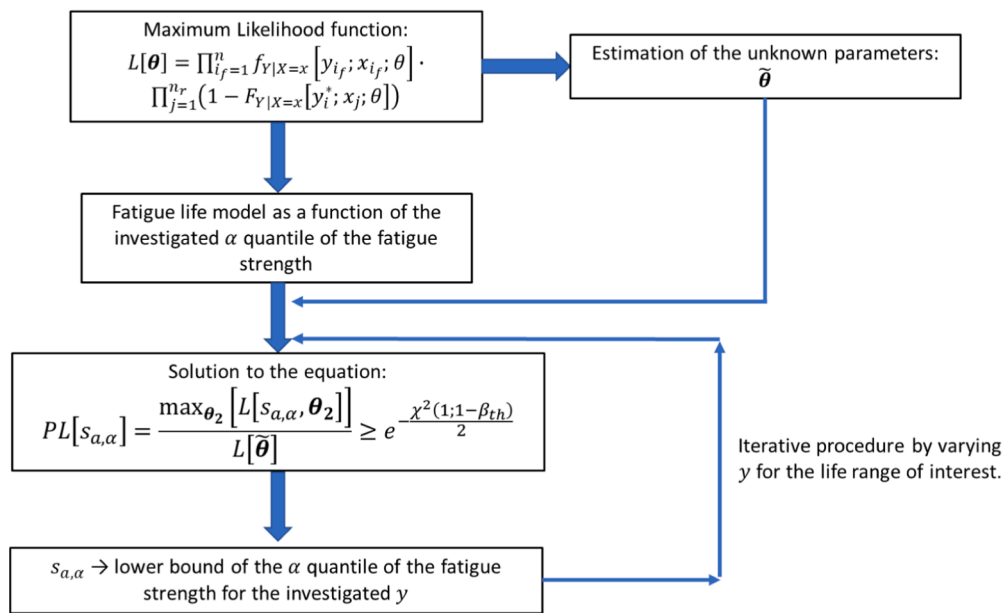
(a)

(b)

Fig. 1. general methodology for the assessment of the LRCB design curves of datasets with failures originating from defects: a) flow chart recalling the main steps of the procedure; b) examples of the Profile Likelihood function with respect to the quantile of the fatigue strength and estimated design curve.

subscript j refers to the j-th runout data ($j = 1 \cdots, n_r$). In the following, the set of parameters maximizing Eq. (1), i.e., the best-fitting parameters, is denoted with $\widetilde{\boldsymbol{\theta}}$. The second step requires the estimation of the Profile Likelihood function, $PL[\bullet]$ for the investigated number of cycles to failures, according to Eq. (2):

$$PL[s_{a,\alpha}] = \frac{\max_{\boldsymbol{\theta}_2}\left[L[s_{a,\alpha}, \boldsymbol{\theta}_2]\right]}{L[\widetilde{\boldsymbol{\theta}}]} \geq e^{-\frac{\chi^2(1;1-\beta_{th})}{2}} \tag{2}$$

being $\boldsymbol{\theta}_2$ the set of the model parameters, according to [10], $L[\widetilde{\boldsymbol{\theta}}]$ the Likelihood function computed for $\widetilde{\boldsymbol{\theta}}$, $\chi^2(1; 1 - \beta_{th})$ the $(1 - \beta_{th})$-th quantile of a Chi-square distribution with 1 degree of freedom and $s_{a,\alpha}$ is the α-th quantile of the fatigue strength at the investigated number of cycles to failure. Practically, by varying $s_{a,\alpha}$ in a reasonable range, the $PL[s_{a,\alpha}]$ function is built point by point. The $s_{a,\alpha}$ values solving Eq. (2) are the lower and the upper bound of the $(1 - \beta_{th})\%$ Likelihood Ratio Confidence Interval for the investigated α quantile of the fatigue strength. However, since the lower bound of the confidence interval is to be assessed in the present work, the lower one-sided confidence bound is considered, i.e., $1 - \beta_{th}$ must be replaced with $(2 \bullet \alpha_C - 1)$, being α_C the confidence level of interest [10]. According to Eq. (1) and [10], the Likelihood function must be expressed as a function of the quantile of the fatigue strength of interest, $s_{a,\alpha}$. This can be achieved by manipulating and rearranging the model for the statistical distribution of the fatigue life, as detailed in the following sections. The design curve is finally obtained by solving Eq. (2) for the range of y of interest.

Fig. 1 helps clarifying the methodology followed for the estimation of the design curve with the LRCB: Fig. 1a is a flow chart recalling the main steps of the procedure developed for assessing the lower bound of the quantile of the fatigue strength. Fig. 1b shows an example of the Profile Likelihood function with respect to the quantile of the fatigue strength and a design curve for a dataset showing a linear decreasing trend. For further details on this procedure, the reader is referred to [10].

2.2. Linear decreasing trend: Conditional P-S-N curves

The simplest statistical model proposed by the Authors for modelling the influence of defects on the fatigue response is the one reported in Eq. (3), to be used for datasets showing a linear decreasing trend in the S-N plot. According to Eq. (3), the cumulative distribution function (cdf) of the fatigue life, $F_{Y|\sqrt{a_{d,0}}}(y; x, \sqrt{a_{d,0}})$, is conditioned to the logarithm of the applied stress amplitude ($x = \log_{10}(s_a)$) and to the logarithm of the defect size, $\sqrt{a_{d,0}}$. The fatigue life is assumed to be Normally distributed, with constant standard deviation σ_Y and mean $\mu_Y(x, \sqrt{a_{d,0}})$ linearly dependent on x and on $\log_{10}(\sqrt{a_{d,0}})$, according to [5,34]:

$$\begin{aligned}F_{Y|\sqrt{a_{d,0}}}(y; x, \sqrt{a_{d,0}}) &= \Phi\left(\frac{y - \mu_Y(x, \sqrt{a_{d,0}})}{\sigma_Y}\right) \\ &= \Phi\left(\frac{y - (c_Y + m_Y \bullet \log_{10}(s_a) + n_Y \bullet \log_{10}(\sqrt{a_{d,0}}))}{\sigma_Y}\right)\end{aligned} \tag{3}$$

The constant coefficients c_Y, m_Y and n_Y are estimated by applying the Maximum Likelihood Principle (Eq. (1)). By solving Eq. (3) for the α-th quantile of interest, the P-S-N curve conditioned to a defect with characteristic size equal to $\sqrt{a_{d,0}}$ can be estimated.

To assess the design curve for the conditional linear P-S-N model, Eq. (3) should be rearranged to express the Profile Likelihood as a function of $s_{a,\alpha}$. For example, the constant coefficient c_Y can be obtained from the expression of the α-th quantile of the fatigue strength:

$$c_Y = y_\alpha - \Phi^{-1}(\alpha) \bullet \sigma_Y - m_Y \bullet \log_{10}(s_{a,\alpha}) - n_Y \bullet \log_{10}(\sqrt{a_{d,0}}) \tag{4}$$

being $y_\alpha = \log_{10}(n_{f,\alpha})$ the logarithm of the considered number of cycles

to failure, $n_{f,\alpha}$. By replacing Eq. (4) in Eq. (3), an expression for the fatigue life distribution as a function of the α-th quantile of the fatigue strength, $s_{a,\alpha}$, can be obtained and exploited for the estimation of the design curve by solving Eq. (2) for different y_α values, with $\boldsymbol{\theta}_2 = (m_Y, n_Y, \sigma_Y)$.

2.3. Linear decreasing trend: Marginal P-S-N curves

In [31–33], the Authors introduced the so-called "Marginal P-S-N curves", i.e., the conditional P-S-N curves marginalized over the distribution of the defect size, $\sqrt{A_{d,0}}$, that is assumed to follow a Largest Extreme Value Distribution (LEVD), according to [5]. In this way, the dependence between the P-S-N curve and the defect size is eliminated, with the P-S-N curve "averaged" over the LEVD distribution. This model has been exploited for the analysis of the results of ultrasonic VHCF fatigue tests on specimens produced through traditional [31,33] and AM processes showing a linear decreasing trend [35] in the S-N plot. Eq.5 reports the cdf of the marginal fatigue life model, $F_Y(y; x)$:

$$F_Y(y; x) = \int_0^\infty F_{Y|\sqrt{a_{d,0}}}(y; x, \sqrt{a_{d,0}}) f_{\sqrt{A_{d,0}}}(\sqrt{a_{d,0}}) \bullet d\sqrt{a_{d,0}} \tag{5}$$

being $f_{\sqrt{A_{d,0}}}(\sqrt{a_{d,0}})$ the pdf of the random variable $\sqrt{A_{d,0}}$. The set of unknown parameters for the marginal distribution of the fatigue life is the same involved in the conditional fatigue life, i.e., $\boldsymbol{\theta} = (c_Y, m_Y, n_Y \sigma_Y)$. The location and scale parameters of the LEVD are estimated by analysing the fracture surfaces of specimens subjected to fatigue tests or through micro-CT inspections. In order to express the Profile Likelihood function as a function of $s_{a,\alpha}$, one of the unknown parameters, e.g., the c_Y parameter, should be expressed as a function of $s_{a,\alpha}$. However, differently from the conditional model (Eq. (3), the dependence between c_Y and $s_{a,\alpha}$ cannot be expressed in a closed form. Accordingly, for given α, y_α and $s_{a,\alpha}$ values, the c_Y value can be estimated numerically by solving Eq. (5). The computed c_Y value can be inserted in Eq. (5) and then in Eq. (2), allowing for the estimation of the $PL[s_{a,\alpha}]$ function. The steps described in Section 2.1 are then followed.

2.4. Linear decreasing trend and fatigue limit: Marginal P-S-N curves

The marginal P-S-N curve can be exploited also for modelling the fatigue response of datasets showing a linear decreasing trend ending with a horizontal asymptote, i.e., with a fatigue limit. The model described in Section 2.3 should be modified by also considering the statistical distribution of the fatigue limit. Eq. (6) reports the cdf of the marginal fatigue life with a linear decreasing trend and a fatigue limit:

$$\begin{aligned}F_Y(y; x) = \int_0^\infty &F_{Y|\sqrt{a_{d,0}}}(y; x, \sqrt{a_{d,0}}) \bullet F_{X_l|\sqrt{a_{d,0}}}(x; \sqrt{a_{d,0}}) \bullet f_{\sqrt{A_{d,0}}}(\sqrt{a_{d,0}}) \\ &\bullet d\sqrt{a_{d,0}}\end{aligned} \tag{6}$$

being $F_{X_l|\sqrt{a_{d,0}}}(x; \sqrt{a_{d,0}})$ the cdf of the logarithm of the fatigue limit random variable, $X_l|\sqrt{a_{d,0}}$, which is assumed to follow a Normal distribution with constant deviation σ_{X_l} and mean $\mu_{X_l}(\sqrt{a_{d,0}})$ reported in Eq. (7):

$$\mu_{X_l}(\sqrt{a_{d,0}}) = \frac{c_{sl} \bullet c_{th} \bullet (HV + 120)}{(\sqrt{a_{d,0}})^{0.5 - \alpha_{th}}} \tag{7}$$

being c_{sl}, c_{th} and α_{th} constant coefficients to be estimated from the experimental data and HV the material Vickers hardness. To summarize, the set of parameters to be estimated with the Maximum Likelihood Principle for this model is $\boldsymbol{\theta} = (m_Y, c_Y, n_Y, \sigma_Y, c_{sl}, c_{th}, \alpha_{th}, \sigma_{X_l})$. In order to compute the lower bound of the fatigue strength from Eq. (1), one of the
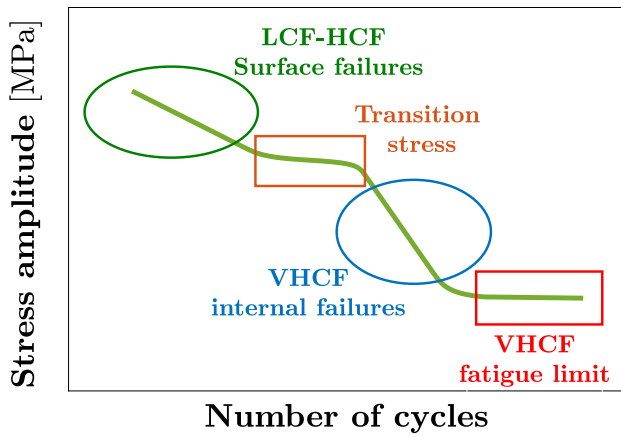
Fig. 2. example of duplex S-N curve, with the failure modes highlighted [37].

constant coefficients in the set of parameters included in θ should be expressed as a function of the α quantile of the fatigue strength. For example, the m_Y coefficient can be computed numerically for given α, y_α and $s_{a,\alpha}$ values. By replacing the computed m_Y value in Eq. (6) and then in Eq. (2), the Profile Likelihood as a function of $s_{a,\alpha}$ is obtained. Accordingly, for this model, $\theta_2 = \left(c_Y, n_Y, \sigma_Y, c_{sl}, c_{th}, \alpha_{th}, \sigma_{X_l} \right)$.

2.5. Duplex P-S-N curves

The last model is the one allowing to assess the P-S-N curves with failures in the LCF-VHCF life range and showing a duplex trend, according to [23,36]. This is the most general model for the fatigue life, and it is characterized by a first slope in the LCF-HCF life region, with surface failures, a transition region with the curve assuming an almost horizontal trend, a second slope in the VHCF life region, with failures originating from defects, and a final asymptote, corresponding to the VHCF limit. In the VHCF life region, fatigue failures originate from defects with the formation of the FGA, allowing for crack propagation from defects characterized by a Stress Intensity Factor (SIF) smaller than the SIF threshold. The stress-life relationship for datasets showing this trend is modelled by considering the statistical distribution of the transition stress, which discriminates between the surface and the internal failure

mode, the statistical distribution of the fatigue life for surface failures in the LCF-HCF life region and the model for the marginal P-S-N curve with fatigue limit (Section 2.4). The cdf of the fatigue life modelling a duplex trend is reported in Eq. (8), according to [26]:

$$F_Y(y;x) = F_{X_t}(x) \bullet F_{Y|surf}(y;x) + \left(1 - F_{X_t}(x)\right) \bullet F_{Y|int}(y;x) \qquad (8)$$

being $F_{Y|int}(y;x)$ the cdf of the fatigue life for internal failures in the VHCF region (corresponding to the cdf reported in Eq. (6), $F_{Y|surf}(y;x)$ the cdf of the fatigue life for surface failures in the LCF-HCF life region, and $F_{X_t}(x)$ the cdf of the transition stress. $F_{Y|surf}(y;x)$ is Normally distributed, with constant standard deviation $\sigma_{Y,surf}$ and mean $\mu_{Y,surf}(x)$ linearly dependent on x $\left(\mu_{Y,surf}(x) = c_{Y,surf} + m_{Y,surf} \bullet x\right)$, being $c_{Y,surf}$ and $m_{Y,surf}$ two constant coefficients). Similarly, $F_{X_t}(x)$ is Normally distributed, with constant mean μ_{X_t} and standard deviation σ_{X_t}. Fig. 2 shows a representative duplex S-N curve, with the different life regions highlighted [37].

The model in Eq. (8) can properly describe the duplex trend, differentiating between the type of failure modes. The set of parameters to be estimated by applying the Maximum Likelihood Principle is $\theta = \left(\mu_{Y,surf}, \sigma_{Y,surf}, \mu_{X_t}, \sigma_{X_t}, \mu_Y, \sigma_Y, \mu_{X_l}, \sigma_{X_l}\right)$. Following the procedure described in Sections 2.3 and 2.4, the μ_{X_t} value is obtained numerically (solving Eq. (8) for given α, y_α and $s_{a,\alpha}$ values). By replacing the computed μ_{X_t} value in Eq. (8) and then in Eq. (2), the Profile Likelihood as a function of $s_{a,\alpha}$ is obtained, with $\theta_2 = \left(\mu_{Y,surf}, \sigma_{Y,surf}, \sigma_{X_t}, \mu_Y, \sigma_Y, \mu_{X_l}, \sigma_{X_l}\right)$. The design curves are finally obtained point by point for the investigated y, according to the procedure detailed in Section 2.1.

3. Design curves with the bootstrap approach

In this section, the second method developed for the estimation of the design curve of datasets failing from defects is described. With this approach, a large number of datasets is simulated starting from the statistical distribution of the fatigue life estimated from the experimental data. For each simulated dataset, the P-S-N curves are estimated and thereafter exploited for the assessment of the design curve. In Section 3.1, the procedure for assessing the design curve of datasets showing a linear decreasing trend (conditional and marginal) and a
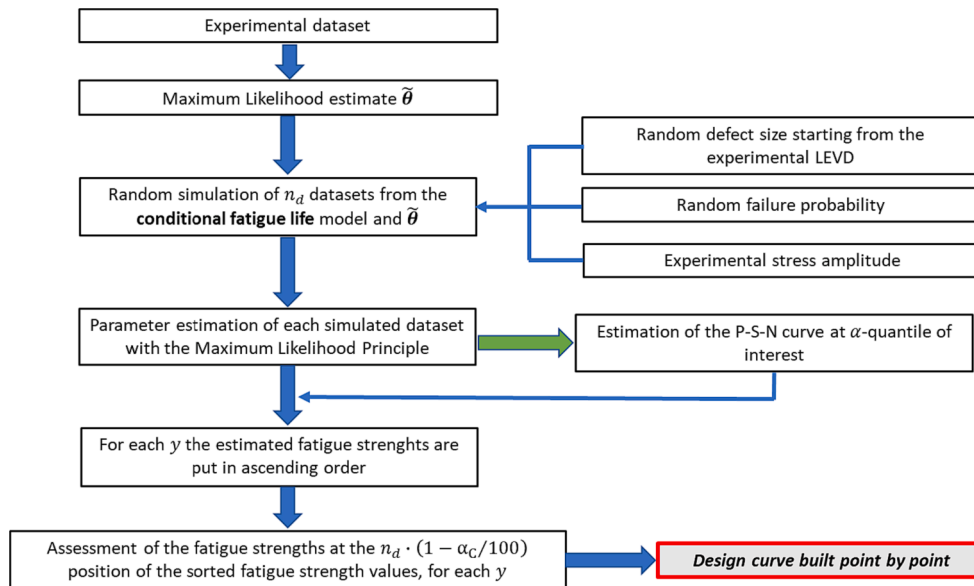

Fig. 3. procedure for the estimation of the design curves (linear decreasing trend and linear decreasing trend and fatigue limit, marginal or conditional) with the bootstrap approach.
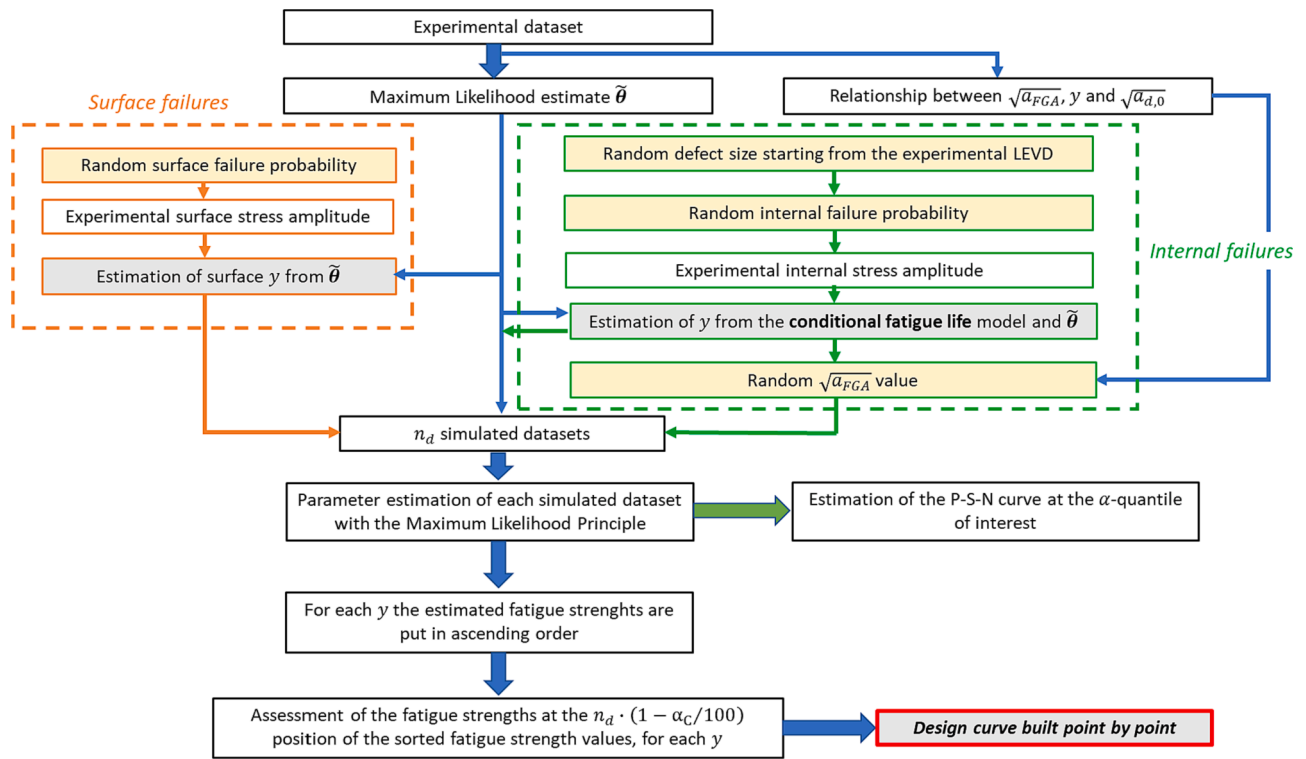
Fig. 4. procedure for the estimation of the duplex design curves with the bootstrap approach.

linear decreasing trend with a fatigue limit (marginal P-S-N curves) is described. Section 3.2, on the other hand, focuses on the steps followed to build the design curve with the bootstrap approach for datasets showing a duplex trend.

3.1. Linear decreasing and linear decreasing trend with fatigue limit: Conditional and marginal model

The flow chart shown in Fig. 3 summarizes the step to be followed for the estimation of the design curves with the bootstrap approach, for datasets showing a linear decreasing trend or a linear decreasing trend with a final asymptote. This procedure can be used regardless of the considered model, marginal or conditional, since the only difference is the statistical distribution considered for the parameter estimation and the simulation of random data, as detailed in the following.

According to Fig. 3, the first step of the proposed procedure involves the estimation of the set unknown material parameters of the cdf of the fatigue life considered for fitting the experimental data. Secondly, a random defect size is simulated by considering the experimental LEVD, that is the LEVD whose parameters are estimated by considering the defects at the originating fatigue failures. Concurrently, a random failure probability is simulated. Starting from the simulated defect size and the random failure probability, for each experimental stress amplitude, the corresponding y is simulated from the cdf of the conditional fatigue life (Section 2.2) with $\theta = \widetilde{\theta}$. For the linear decreasing trend, the model in Eq. (3) is to be considered. On the other hand, for the model with linear trend and fatigue limit, the model in Eq. (9) (conditional P-S-N curve describing a linear decreasing trend and the fatigue limit) must be considered:

$$F_{Y|int}(y;x) = F_{Y|\sqrt{a_{d,0}}}\left(y;x,\sqrt{a_{d,0}}\right) \bullet F_{X_l|\sqrt{a_{d,0}}}\left(x_l;\sqrt{a_{d,0}}\right) \qquad (9)$$

By repeating this procedure for the stress amplitudes of the original datasets, a dataset replicating the original one is simulated. It must be noted that the simulated y are limited to the runout number of cycles considered for the experimental tests. By iteratively repeating this

operation, n_d datasets are randomly simulated. For each of the n_d datasets, the material parameters are estimated by applying the Maximum Likelihood Principle and the P-S-N curve at the investigated α quantile is obtained. For the marginal cdf model, the LEVD is moreover estimated for each n_d dataset by considering the simulated defect sizes, thus accounting also for the variability of the defect size with the LEVD. Finally, the estimated fatigue strengths at each y are sorted in ascending order. The fatigue strength at the $n_d \bullet (1 - \alpha_C/100)$ position corresponds to the lower bound fatigue strength, i.e., the design curve.

3.2. Duplex P-S-N curves

The procedure for the estimation of the duplex design curve with the bootstrap approach is more complex, since the random occurrence of surface and internal failures should be considered. Fig. 4 shows the flow chart of the procedure developed for the assessment of the bootstrap design curve.

According to Fig. 4, the first step of the procedure involves the assessment of the Maximum Likelihood estimates from the experimental data. In this phase, the relationship between the square root of the FGA, $\sqrt{a_{FGA}}$, the initial defect size, and y must be experimentally assessed [38]. A Normal distribution has been considered for the $\sqrt{A_{FGA}}$ random variable, to model also its experimental variability, according to Eq. (10):

$$F_{\sqrt{A_{FGA}}}\left(\sqrt{a_{FGA}};n_f,\sqrt{a_{d,0}}\right) = \Phi\left(\frac{\sqrt{a_{FGA}} - \mu_{\sqrt{A_{FGA}}}\left(n_f,\sqrt{a_{d,0}}\right)}{\sigma_{\sqrt{A_{FGA}}}}\right) \qquad (10)$$

with $\mu_{\sqrt{A_{FGA}}}(n_f,\sqrt{a_{d,0}}) = c_{\sqrt{A_{FGA}}} + m_{\sqrt{A_{FGA}}} \bullet \log_{10}(n_f) + n_{\sqrt{A_{FGA}}} \bullet \log_{10}(\sqrt{a_{d,0}})$, being $c_{\sqrt{A_{FGA}}}$, $m_{\sqrt{A_{FGA}}}$ and $n_{\sqrt{A_{FGA}}}$ material parameters to be estimated from the experimental data, and $\sigma_{\sqrt{A_{FGA}}}$ corresponding to the standard deviation. These unknown parameters are estimated through a multiple linear regression. Thereafter, a random failure probability and a random defect size, starting from the experimental LEVD, are simulated. By considering the stress amplitude levels
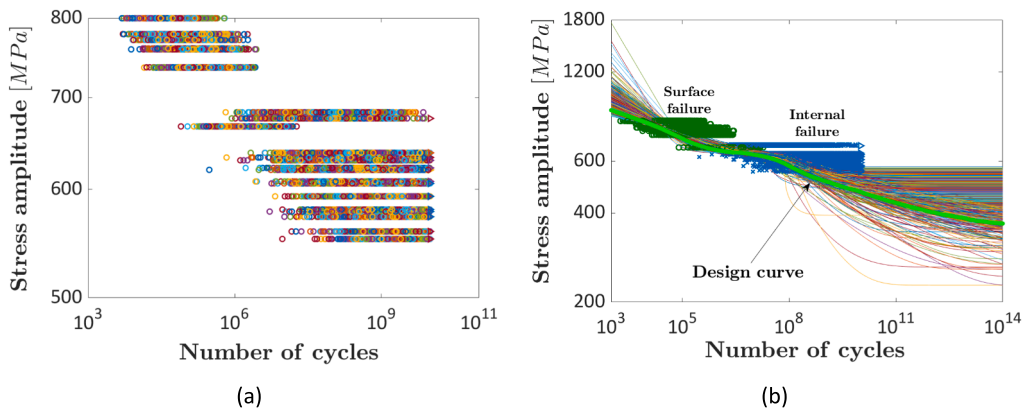
Fig. 5. Bootstrap method applied to the duplex P-S-N curve model: a) simulated datasets; b) estimated P-S-N curves for each simulated dataset and design curve.

of failures originating from defects, the random y for each internal failure is simulated according to the conditional model reported in Eq. (9).

The fatigue life for stress amplitudes inducing surface failures is, on the other hand, simulated starting from the cdf of the fatigue life for surface failures and by considering simulated random surface failure probabilities. The simulated fatigue life is limited to the experimental runout number of cycles to failure.

By combining the applied stress amplitude and the simulated fatigue life for surface and internal failures, n_d datasets replicating the experimental one are simulated. According to [31], the relationship between the SIF associated with the FGA and the FGA size should be estimated for modelling the crack nucleation when the FGA forms and assessing the fatigue limit distribution. For each simulated dataset, this dependence is obtained by considering the $\sqrt{a_{FGA}}$ values estimated with Eq. (10) for the simulated defect sizes and the experimental $c_{\sqrt{A_{FGA}}}$, $m_{\sqrt{A_{FGA}}}$, $n_{\sqrt{A_{FGA}}}$ and $\sigma_{\sqrt{A_{FGA}}}$. Thereafter, the unknown parameters for each simulated dataset can be obtained by applying the Maximum Likelihood Principle. Finally, the same steps described in Section 3.2 are followed. In particular, the P-S-N curves at the investigated α quantile are obtained for the simulated datasets and the fatigue strengths at each y are sorted in ascending order. The fatigue strengths at the $n_d \bullet (1 - \alpha_C / 100)$ position are the lower bound fatigue strengths, i.e., the P-S-N design curve.

Fig. 5 shows an example of $n_d = 1000$ datasets estimated for the duplex model, whereas Fig. 5b shows the estimated P-S-N curve for each simulated dataset, together with the design curve (green curve).

4. Design curve: Experimental validation

In this section, the methodologies described in Section 2 and Section 3 for the estimation of the design curve from datasets with failures originating from defects are validated on experimental data obtained by the Authors or on literature datasets. The linear model (conditional and marginal) has been validated on AM AlSi10Mg data obtained by the Authors (Sections 4.1 and 4.2, respectively). The marginal P-S-N curve describing a linear trend ending with an asymptote is validated with the experimental data in [21] (Section 4.3). Finally, the experimental data for validating the design P-S-N curves with a duplex trend are obtained by combining literature data (in the LCF-HCF life regions, with surface failures) and experimental data obtained by the Authors, in the VHCF life region (Section 4.4). The validity of the two proposed approaches, their strength and weaknesses are finally discussed in Section 4.5. The design curve is assumed as the R90C90 P-S-N curves, according to the industrial practice [4].

The literature data considered for the validation have been digitized with the software ENGAUGE® by considering the S-N plot reported in the original paper, if not available in tabular form. Digitization error, even if limited, cannot be excluded or eliminated. However, it must be noted that the aim of this work is to qualitatively validate the proposed models and compare the design curves obtained with different approaches, thus digitization errors are not expected to have a significant influence on this analysis.
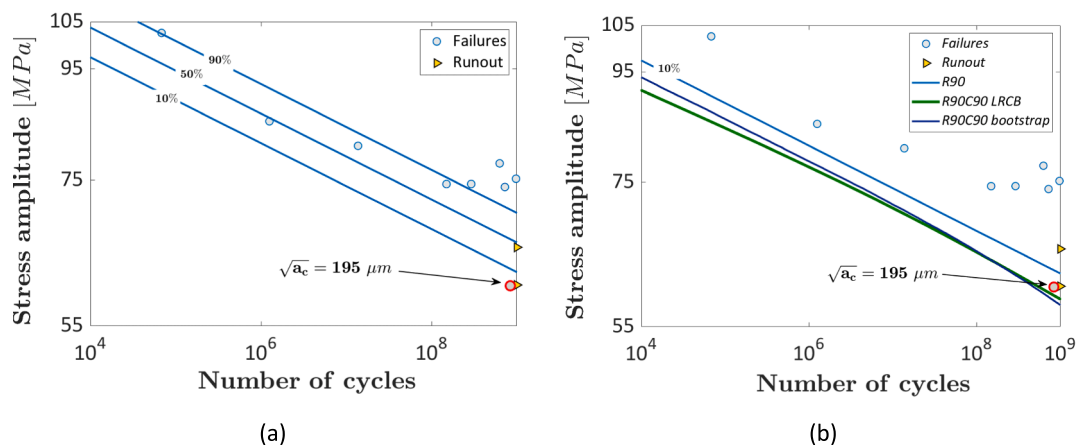

Fig. 6. Validation of the model for the conditional P-S-N design curves by considering a defect with $\sqrt{a_{d,0}} = 195\mu m$: a) median, 0.1-th and 0.9-th quantiles P-S-N curves; b) 0.1-th and design P-S-N curves estimated with the LRCB and the bootstrap approach.
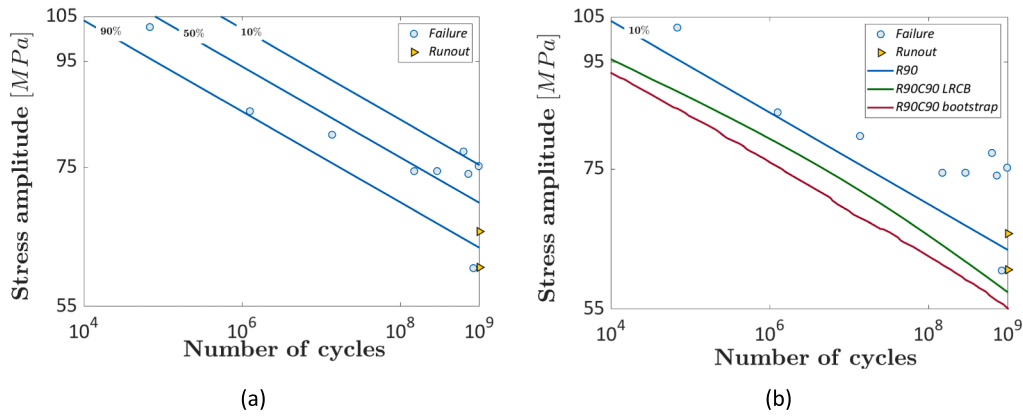
(a)   (b)

Fig. 7. validation of the model for marginal P-S-N design curves for datasets showing a linear decreasing trend: a) median, 0.1-th and 0.9-th quantile P-S-N curves; b) 0.1-th and design P-S-N curves estimated with the LRCB and the bootstrap approach.

4.1. Conditional linear decreasing trend: Validation on AlSi10Mg data

The model for the conditional P-S-N design curve has been validated on experimental data obtained by the Authors [35] by testing AlSi10Mg specimens with large risk-volume [5], $V_{90} = 2300\,mm^3$, and produced through a Selective Laser Melting (SLM) process. The specimens have been built in horizontal direction and tested after mechanical polishing and without subsequent heat treatment. Ultrasonic fatigue tension–compression tests have been carried out up to 10^9 cycles (runout number of cycles to failure). The defects at the origin of the fatigue failures have been observed on the fracture surfaces and their characteristic size has been assessed according to the indications provided in [5,21]. The conditional P-S-N curves have been estimated for the second-largest defect found experimentally and characterized by $\sqrt{a_{d,0}} = 195\,\mu m$. This defect has induced a failure at an applied stress amplitude level (failure at about $9 \cdot 10^8$ cycles at 60MPa), significantly smaller than that of the other tested specimens (all failures above 70MPa). Fig. 6a shows the conditional P-S-N curves (median, 0.1-th and 0.9-th) estimated by considering the second largest defect, whereas Fig. 6b shows the 0.1-th quantile P-S-N curve and the design curves estimated with the LRCB and with the bootstrap approach.

According to Fig. 6a, the failure originating from the investigated defect is not included within the 0.9-th and the 0.1-th P-S-N curves. The 0.1-th quantile curve is non-conservatively above this anomalous failure. A P-S-N quantile curve with significantly higher reliability (e.g., 0.01-th) should be therefore considered to ensure an appropriate safety margin. On the other hand, the R90C90 P-S-N curves estimated with the LRCB and the bootstrap method are below this experimental failure,

showing the same trend and with limited differences. This analysis proves the importance of modelling the lower confidence bound of a specific quantile P-S-N curve, especially for design purposes and when reliable safety margins with respect to failures are required. Indeed, failures at unexpected low-stress amplitudes may occur when defects drive the fatigue response and high-reliability quantiles may not meet the safety standard requirement, depending on the application.

4.2. Marginal linear decreasing trend: Validation on AlSi10Mg data

The model for the design marginal P-S-N curves for datasets showing a linear decreasing trend has been validated on the AlSi10Mg data obtained by the Authors [35] (horizontal mechanically polished specimens with large risk-volume and tests up to 10^9 cycles). Fig. 7a shows the median, the 0.1-th and the 0.9-th P-S-N curves, together with the experimental data. Fig. 7b shows the 0.1-th P-S-N curve and the R90C90 P-S-N curves estimated with LRCB and with the bootstrap approach.

According to Fig. 7a, the estimated marginal P-S-N curves are in good agreement with the experimental data, with the median curve almost equally subdividing the experimental failures. The 0.1-th P-S-N curve is below all the experimental failures, except for the experimental failure showing an anomalous behaviour and failing at low-stress amplitude due to a large defect (Section 4.1). The large experimental scatter and the possible occurrence of anomalous failures are, on the other hand, accounted for by the design P-S-N curves. Indeed, the design curves estimated with LRCB and bootstrap approaches are conservatively below all the experimental failures and show similar trends. The bootstrap design curve is however more conservative and below the LRCB
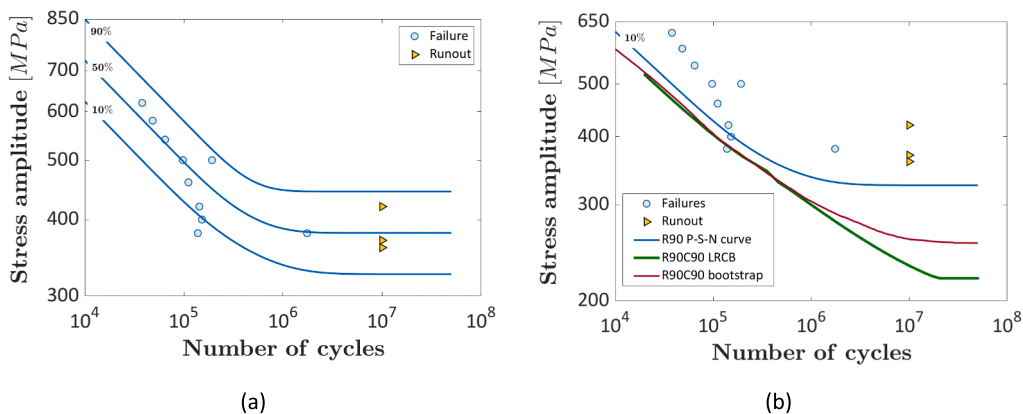

(a)   (b)

Fig. 8. validation of the model for marginal P-S-N design curves for datasets showing a linear decreasing trend and a fatigue limit: a) median, 0.1-th and 0.9-th quantiles P-S-N curves; b) 0.1-th and design P-S-N curves estimated with the LRCB and the bootstrap approach.
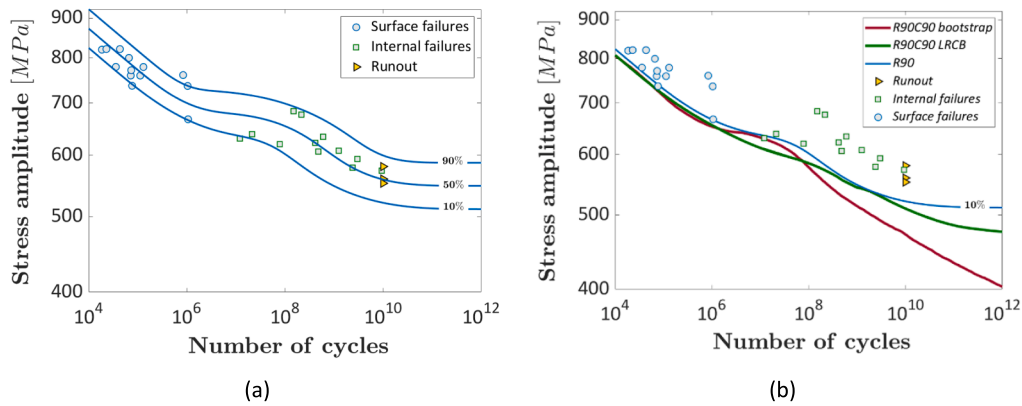
Fig. 9. validation of the duplex P-S-N design curves for datasets showing a duplex in the LCF-VHCF life range: a) median, 0.1-th and 0.9-th quantile P-S-N curves; b) 0.1-th and design P-S-N curves estimated with the LRCB and the bootstrap approach.

design curves. By comparing Fig. 6b and 7b, the marginal design curves are more conservative, since they provide a larger safety margin with respect to the anomalous failure at 60MPa.

The conditional and the marginal P-S-N design curves have proven to be effectively used for a reliable fatigue design, ensuring an appropriate safety margin with respect to failures, even if originating from unexpected large defects.

4.3. Marginal linear decreasing trend and fatigue limit: Validation on Ti6Al4V data

The marginal P-S-N curve model describing a linear decreasing trend and a fatigue limit is validated in this section. The experimental data in [21], obtained by testing Ti6Al4V specimens produced through a Direct Metal Laser Sintering (DMLS) process, have been considered for the validation. In [21], rotating bending tests have been carried out up to 10^7 cycles tests on specimens built in vertical direction, mechanically polished with fine-grain sandpaper and subjected after the DMLS process to a stress relief heat treatment. Fig. 8a shows the median, the 0.1-th and the 0.9-th P-S-N curves, together with the experimental data. Fig. 8b shows the 0.1-th P-S-N curve and the R90C90 P-S-N curves estimated with the LRCB and with the bootstrap approach.

According to Fig. 8a, the marginal model describing a linear decreasing trend and fatigue limit is in agreement with the experimental data, with the median P-S-N curve being above about 50% of the experimental failures. The experimental scatter tends to increase with the number of cycles to failure, with the stress amplitude difference between the 0.1-th and the 0.9-th being larger at 10^7 cycles than at 10^4 cycles. This can be ascribed to the different failure numerosity in the investigated life regions, with failures mainly concentrated below 10^5 cycles and only one failure above 10^6 cycles. Two failures are below the 0.1-th quantile P-S-N curve. According to Fig. 8b, the estimated LRCB and the bootstrap design curves are below the 0.1-th P-S-N curve, as expected. All experimental failures, except one, are below the design curves estimated with the two investigated approaches. Accordingly, for this dataset even the R90C90 design curve does not ensure the proper safety level and larger reliability, or confidence levels should be considered to account for the experimental variability caused by defects. The LRCB and the bootstrap design curves show the same trend and are very close in the finite life region where the data show a linear decreasing trend. On the other hand, the difference increases in the infinite life region, with the fatigue limit estimated with LRCB being more conservative. The larger distance between design curves and failures in the infinite life region is due to the limited amount of data in this life range, with the design curves moving downward to account for the estimation uncertainty.

4.4. Duplex P-S-N curves: Validation on H13 data

The duplex P-S-N design curve model has been finally validated on datasets obtained by testing an H13 tool steel. For the LCF-HCF life region, the experimental data in [39], with failures originating from the specimen surface, have been considered. On the other hand, the experimental data collected by the Authors in [40] with ultrasonic fatigue tests have been considered for the VHCF life region. Within this life range, all fatigue failures originated from internal defects, mainly spherical inclusions, surrounded by the FGA. The initial defect and the FGA have been observed and measured with the Scanning Electron Microscope (SEM). It is worth noting that datasets obtained by testing specimens made of the same material but with different characteristics have been considered for this experimental validation. However, the objective of the present section is the validation of the duplex P-S-N curve model, rather than providing the best fitting of experimental data obtained through tests in controlled conditions. Fig. 9a shows the experimental data, together with the estimated P-S-N curves (0.1-th, median and 0.9-th). Fig. 9b plots the 0.1-th quantile P-S-N curve and the design curves estimated with the LRCB and the bootstrap approaches.

According to Fig. 9a, the proposed model for the duplex P-S-N curve is in agreement with the experimental data, with the median curve almost equally subdividing surface and internal failures. The 0.1-th quantile P-S-N curve is below the experimental failures, apart from one surface failure and one internal failure. The LRCB design curve is below the experimental failures, being close to the experimental data in the LCF-HCF life region and farther from failures in the VHCF region. Moreover, it is close to the 0.1-th P-S-N curve between 10^8-10^9 cycles, since failures are significantly above the 0.1-th P-S-N curve. Above 10^{10} cycles, the curve approaches an asymptotic trend, reaching the maximum distance from the 0.1-th P-S-N curve. The bootstrap design curve shows a different trend. In the LCF-HCF life region, the bootstrap design curve overlaps the LRCB design curve and is below all experimental surface failures, as expected. On the other hand, it is close to the 0.1-th quantile P-S-N curve in the region where the transition between surface and internal failures occurs, becoming finally very conservative in the VHCF life region and not approaching an asymptotic trend for the plotted life range of interest, with a large distance from the LRCB design curve. The trend in the "transition region" can be explained by considering the procedure for simulating the datasets. Indeed, for the analyzed dataset, the number of experimental data in the "transition region" is limited and the same occurs for the simulated datasets. Accordingly, the standard deviations of the transition stress distribution tend to be small for the majority of simulated datasets, with possible less conservative trends for the design curve in this life region. However, the design curve estimated with the bootstrap approach is below all experimental failures, as expected.

In general, it can be concluded that both approaches are effective, with the LRCB design curve properly following and adapting to the P-S-N curve trend and the bootstrap design curve being less conservative in the transition region and excessively conservative in the VHCF life region.

5. Discussion

The LRCB and bootstrap approaches have been applied to estimate the design curves of stress-life models developed by the Authors. The procedure for estimating the design curve with the LRCB has been proven effective, with the estimated design curves in good agreement with experimental failures and runout data, even for the dataset showing a duplex trend. The estimated design curves followed the trend of the quantile P-S-N curve of interest, ensuring a reliable safety margin, as expected, and being conservative also for failures originating from unexpected large defects (Figs. 6 and 7). The main drawback in the application of the proposed approach is its implementation complexity. Indeed, an iterative process based on repeated optimizations is required to solve Eq. (2) and to obtain the Profile Likelihood in function of $s_{a,a}$. Moreover, optimization algorithms strongly depend on the initial guess of the unknown parameters, i.e., $\boldsymbol{\theta}_2$, which, if not properly chosen, may provide non-physical estimations of the Profile Likelihood values, especially for the more complicated models (i.e., linear with the fatigue limit and duplex). Accordingly, for each dataset, the initial unknown parameters and the optimization parameters (e.g., type of algorithms, number of iterations, tolerance limits) should be reliably chosen, for example with a trial-and-error strategy, to obtain feasible solutions and reliable estimations.

The methodology based on the bootstrap approach is simpler than that based on the LRCB, since in the first phase random datasets are simulated and in the second phase the quantile of interest P-S-N curve is estimated for each simulated dataset. Differently from [10], in presence of defects at the origin of the fatigue failure, a random defect size is also simulated starting from the experimental LEVD of $\sqrt{A_{d,0}}$. Accordingly, the variability associated to the defect size is also modelled and accounted for. Furthermore, when fatigue failures originate from defects with FGA formation in the VHCF life region, the experimental dependence between the number of cycles, the FGA size and the initial defect has been also experimentally assessed and considered for each simulated dataset, taking into account also the weakening mechanisms allowing for the crack initiation in the VHCF life region. With this approach, no assumptions are to be made on the characteristics of confidence intervals of the investigated quantile (e.g., Normal assumption). The fundamental step for the application of this approach is a proper estimation of the initial parameters $\widetilde{\boldsymbol{\theta}}$ of the fatigue life distribution. This means that the fatigue life distribution estimated from the experimental sample should be as close as possible to the statistical distribution of the original population. However, this is not ensured when datasets with a limited number of data are available. Bias in the original dataset can lead to large errors in the estimation of the P-S-N curves and, accordingly, of the design curves. Moreover, depending on the distribution of failures in the original dataset, the estimated design curve can be more or less conservative in different life regions, as in the duplex model of Section 4.4 (Fig. 9b). The easier implementation procedure is compensated by the larger computational time, if compared to that required for the LRCB design curve.

It must be noted that in the present research a log-normal distribution for the fatigue life has been considered. However, the proposed approach is general and not dependent on the statistical distribution assumed for the fatigue life. Accordingly, different statistical distributions (e.g., the Weibull distribution) can be also reliably employed.

In general, it can be concluded that the proposed approaches are effective and can be employed for the assessment of the design curves for datasets with failures originating from defects. However, differently from the methodologies which do not model the defect influence, the analysis of the experimental results is more complex. The defect at the origin of the fatigue failures should be observed with the SEM to measure its equivalent size. In addition, for failures in the VHCF life region, the FGA size should be also measured. Accounting for the defect size ensures a reliable assessment of the source of the experimental variability and can guarantee a reliable safety margin also with respect to anomalous failures from rare defects (Figs. 6 and 7). The experimental validation has also shown that, for datasets with failures originating from defects, the R90C90 design curve, which is commonly considered for industrial applications, may not ensure an appropriate safety margin, suggesting that higher reliability and confidence levels are necessary. However, as suggested in the International Standards (e.g., ASTM E739 – 10) the reliability and confidence levels should not exceed the 95% value. It must be noted that the Weibull distribution can be also considered for the distribution of the fatigue life, according to the ISO 12107:2012, with literature works [15,16,41] proving that it should be used when the lower bound of the design curve is estimated. However, for the investigated datasets with failures originating from defects, the log-normal distribution has been preferred for its versatility, simplicity, and fitting capabilities and has proven to be reliably employed also for the lower bound of the P-S-N curves [10,37,42], with a thorough validation on experimental data in different testing conditions and life ranges. Accordingly, the choice of the log-normal distribution is not considered critical, even for the estimation of the lower bound of the P-S-N curves at high reliability and confidence levels, and the assumption of a Weibull distribution is not expected to provide significantly different results.

6. Conclusions

In the present paper, two approaches for the estimation of the fatigue design P-S-N curves of datasets failing from defects have been proposed. Indeed, manufacturing defects strongly affect the fatigue response of parts produced through specific manufacturing processes, e.g., through Additive Manufacturing processes, or in a specific fatigue life region, like the Very High Cycle Fatigue (VHCF) life range. The experimental datasets with fatigue failures originated from manufacturing and internal defects generally exhibit large scatter, which must be properly accounted for to ensure the structural integrity of components in service conditions. Accordingly, an approach based on the Likelihood Ratio Confidence Bound (LRCB) and one based on the bootstrap method have been proposed to model the design P-S-N curves and have been validated on literature data. The square root of the area of the defect has been considered as the characteristic defect size.

The following conclusions can be drawn:

1. Both approaches have been proven to model the influence of defects in the S-N plot, with the design curves ensuring a safety margin with respect to failures.
2. The LRCB approach has been found to be flexible and to follow the P-S-N curve trend for all the investigated models, even for the duplex model, with the safety margin depending on the dataset numerosity and its scatter. On the other hand, its implementation is rather complex, requiring an iterative procedure based on repeated optimizations for each considered number of cycles to failure.
3. The bootstrap approach is less complex, even if the random defect size should be also simulated by considering the Large Extreme value Distribution (LEVD) followed by the defect size random variable. The simulation and the following estimation phase, on the other, can be computationally expensive, depending on the model complexity. Moreover, depending on the distribution of failures in the original dataset, the estimated design curve can be more or less conservative in different life regions, as highlighted in the duplex model close to the transition stress.

Table A1

experimental data considered for the validation of the duplex model (Section 4.4).

Number of cycles	Stress amplitude [MPa]	Failure type
1.86E + 04	820	Surface
2.30E + 04	821	Surface
3.58E + 04	779	Surface
4.33E + 04	821	Surface
6.62E + 04	800	Surface
7.20E + 04	759	Surface
7.36E + 04	771	Surface
7.67E + 04	737	Surface
1.12E + 05	759	Surface
1.30E + 05	779	Surface
8.40E + 05	760	Surface
1.04E + 06	736	Surface
1.06E + 06	667	Surface
1.26E + 09	608	Internal
6.03E + 08	633	Internal
3.02E + 09	593	Internal
1.00E + 10	580	Internal
4.79E + 08	606	Internal
4.17E + 08	622	Internal
7.76E + 07	620	Internal
1.20E + 07	630	Internal
2.19E + 08	676	Internal
2.14E + 07	638	Internal
1.51E + 08	683	Internal
2.40E + 09	578	Internal
1.00E + 10	559	Internal
9.33E + 09	573	Internal
1.00E + 10	552	Internal

4. The R90C90 design curve (reliability and confidence levels equal to 90%), which is generally employed in industrial practice, may not be sufficient to ensure a reliable safety margin in datasets with failures originating from defects, characterized by large variability. Larger reliability and confidence levels, not exceeding the 95% levels, according to the International Standards, are therefore suggested for a reliable design of components for which defects control the fatigue response.

CRediT authorship contribution statement

A. Tridello: Conceptualization, Methodology, Formal analysis, Validation, Writing – original draft. **C. Boursier Niutta:** Data curation, Visualization, Writing – review & editing. **M. Rossetto:** Writing – review & editing, Supervision. **F. Berto:** Writing – review & editing, Supervision. **D.S. Paolino:** Conceptualization, Methodology, Writing – review & editing, Supervision.

Declaration of Competing Interest

The authors declare that they have no known competing financial interests or personal relationships that could have appeared to influence the work reported in this paper.

Data availability

The data used for the validation of the statistical method have been retrieved from published papers. These data are already available in the literature. New data have not been generated in the paper.

Appendix 1

The experimental data in Section 4.1, 4.2 are available in Tabular form in [43]. The experimental data in Section 4.3 are available in tabular form in [21]. The experimental data considered for the validation of th duplex model are available in Table A1 (runout number of cycles to failure 10^{10} cycles). [39,40].

References

[1] BS ISO12107:2003. Metallic materials — Fatigue testing — Statistical planning and analysis of data 2003.

[2] ASTM E739 - 10. Standard Practice for Statistical Analysis of Linear or Linearized Stress-Life (S–N) and Strain-Life (e-N) Fatigue Data 2015.

[3] RI S, A F, RR S, H. F. Metal Fatigue in Engineering. 2000, Wiley. Wiley; 2000.

[4] Li Lee Y, Pan J, Hathaway R, Barkey M. Fatigue testing and analysis: theory and practice, elsevier butterworth- heinemann: New York (USA). New York: Elsevier B. V; 2005.

[5] Murakami Y. Metal fatigue: effects of small defects and nonmetallic inclusions. Elsevier; 2002.

[6] Collins J. Failure of materials in mechanical design—analysis, prediction, and prevention. Wiley; 2021.

[7] Fatemi A, Plaseied A, Khosrovaneh AK, Tanner D. Application of bi-linear log-log S-N model to strain-controlled fatigue data of aluminum alloys and its effect on life predictions. Int J Fatigue 2005;27:1040–50. https://doi.org/10.1016/j.ijfatigue.2005.03.003.

[8] Sonsino CM. Fatigue testing under variable amplitude loading. Int J Fatigue 2007;29:1080–9. https://doi.org/10.1016/j.ijfatigue.2006.10.011.

[9] Paolino DS, Chiandussi G, Rossetto M. A unified statistical model for S-N fatigue curves: Probabilistic definition. Fatigue Fract Eng Mater Struct 2013;36:187–201. https://doi.org/10.1111/j.1460-2695.2012.01711.x.

[10] Tridello A, Boursier Niutta C, Berto F, Tedesco MM, Plano S, Gabellone D, et al. Design against fatigue failures: Lower bound P-S-N curves estimation and influence of runout data. Int J Fatigue 2022;162:106934.

[11] Loren S. Fatigue limit estimated using finite lives´. Fatigue Fract Eng Mater Struct 2003;26(9):757–66.

[12] Pascual FG, Meeker WQ, Meeker WQ. Estimating Fatigue Curves With the Random Fatigue-Limit Model 1999;41:277–90.

[13] Makkonen M. Predicting the total fatigue life in metals. Int J Fatigue 2009;31:1163–75. https://doi.org/10.1016/j.ijfatigue.2008.12.008.

[14] Leonetti D, Maljaars J, Snijder HH. Bert. Fitting fatigue test data with a novel S-N curve using frequentist and Bayesian inference. Int J Fatigue 2017;105:128–43. https://doi.org/10.1016/j.ijfatigue.2017.08.024.

[15] Castillo E, Fernandez-Canteli A. A unified statistical methodology for modeling fatigue damage. Springer; 2009.

[16] Fernández-Canteli A, Castillo E, Blason S, Correia JAFO, De Jesus AMP. Generalization of the Weibull probabilistic compatible model to assess fatigue data into three domains: LCF. HCF and VHCF 2022:159. https://doi.org/10.1016/j.ijfatigue.2022.106771.

[17] Strzelecki P. Determination of fatigue life for low probability of failure for different stress levels using 3-parameter Weibull distribution. Int J Fatigue 2021;145. https://doi.org/10.1016/j.ijfatigue.2020.106080.

[18] Williams CR, Lee YL, Rilly JT. A practical method for statistical analysis of strain-life fatigue data. Int J Fatigue 2003;25:427–36. https://doi.org/10.1016/S0142-1123(02)00119-6.

[19] Sanaei N, Fatemi A. Defects in additive manufactured metals and their effect on fatigue performance: A state-of-the-art review. Prog Mater Sci 2021;117:100724. https://doi.org/10.1016/j.pmatsci.2020.100724.

[20] Zerbst U, Bruno G, Buffière J-Y, Wegener T, Niendorf T, Wu T, et al. Damage tolerant design of additively manufactured metallic components subjected to cyclic loading: State of the art and challenges. Prog Mater Sci 2021;121:100786.

[21] Masuo H, Tanaka Y, Morokoshi S, Yagura H, Uchida T, Yamamoto Y, et al. Influence of defects, surface roughness and HIP on the fatigue strength of Ti-6Al-4V manufactured by additive manufacturing. Int J Fatigue 2018;117:163–79.

[22] Shiozawa K, Lu L, Ishihara S. S-N curve characteristics and subsurface crack initiation behaviour in ultra-long life fatigue of a high carbon-chromium bearing steel. Fatigue Fract Eng Mater Struct 2001;24:781–90. https://doi.org/10.1046/j.1460-2695.2001.00459.x.

[23] Sakai T, Lian B, Takeda M, Shiozawa K, Oguma N, Ochi Y, et al. Statistical duplex S-N characteristics of high carbon chromium bearing steel in rotating bending in very high cycle regime. Int J Fatigue 2010;32(3):497–504.

[24] Tridello A, Boursier Niutta C, Rossetto M, Berto F, Paolino DS. Statistical models for estimating the fatigue life, the stress–life relation, and the P-S–N curves of

metallic materials in Very High Cycle Fatigue: A review. Fatigue Fract Eng Mater Struct 2022;45:332–70. https://doi.org/10.1111/ffe.13610.

[25] Sanaei N, Fatemi A. Defect-based fatigue life prediction of L-PBF additive manufactured metals. Eng Fract Mech 2021;244:107541. https://doi.org/10.1016/j.engfracmech.2021.107541.

[26] Tridello A, Boursier Niutta C, Berto F, Qian G, Paolino DS. Fatigue failures from defects in additive manufactured components: A statistical methodology for the analysis of the experimental results. Fatigue Fract Eng Mater Struct 2021;44:1944–60. https://doi.org/10.1111/ffe.13467.

[27] Murakami Y, Takagi T, Wada K, Matsunaga H. Essential structure of S - N curve : Prediction of fatigue life and fatigue limit of defective materials and nature of scatter. Int J Fatigue 2021;146:106138. https://doi.org/10.1016/j.ijfatigue.2020.106138.

[28] Romano S, Brückner-Foit A, Brandão A, Gumpinger J, Ghidini T, Beretta S. Fatigue properties of AlSi10Mg obtained by additive manufacturing: Defect-based modelling and prediction of fatigue strength. Eng Fract Mech 2018;187:165–89. https://doi.org/10.1016/j.engfracmech.2017.11.002.

[29] Tridello A, Paolino DS, Rossetto M. Ultrasonic VHCF tests on very large specimens with risk-volume up to 5000 mm3. Appl Sci 2020:10. https://doi.org/10.3390/app10072210.

[30] Invernizzi S, Montagnoli F, Carpinteri A. Experimental evidence of specimen-size effects on en-aw6082 aluminum alloy in vhcf regime. Appl Sci 2021:11. https://doi.org/10.3390/app11094272.

[31] Paolino DS, Tridello A, Chiandussi G, Rossetto M. S-N curves in the very-high-cycle fatigue regime: statistical modeling based on the hydrogen embrittlement consideration. Fatigue Fract Eng Mater Struct 2016;39(11):1319–36.

[32] Paolino DS, Tridello A, Chiandussi G, Rossetto M. Estimation of P-S-N curves in very-high-cycle fatigue: Statistical procedure based on a general crack growth rate model. Fatigue Fract Eng Mater Struct 2018;41:718–26. https://doi.org/10.1111/ffe.12715.

[33] Tridello A, Paolino DS, Chiandussi G, Rossetto M. Effect of electroslag remelting on the VHCF response of an AISI H13 steel. Fatigue Fract Eng Mater Struct 2017;40:1783–94. https://doi.org/10.1111/ffe.12696.

[34] Schuller R, Fitzka M, Irrasch D, Tran D, Pennings B, Mayer H. VHCF properties of nitrided 18Ni maraging steel thin sheets with different Co and Ti content. Fatigue Fract Eng Mater Struct 2015;38:518–27. https://doi.org/10.1111/ffe.12251.

[35] Tridello A, Biffi CA, Fiocchi J, Bassani P, Chiandussi G, Rossetto M, et al. VHCF response of as-built SLM AlSi10Mg specimens with large loaded volume. Fatigue Fract Eng Mater Struct 2018;41(9):1918–28.

[36] Lu LT, Zhang JW, Shiozawa K. Influence of inclusion size on S-N curve characteristics of high-strength steels in the giga-cycle fatigue regime. Fatigue Fract Eng Mater Struct 2009;32:647–55. https://doi.org/10.1111/j.1460-2695.2009.01370.x.

[37] Tridello A, Niutta CB, Berto F, Rossetto M, Paolino DS. Duplex LCF-VHCF P-S-N design curves: a methodology based on the Maximum Likelihood Principle. Procedia Struct Integr 2022;42:1320–7. https://doi.org/10.1016/j.prostr.2022.12.168.

[38] Chapetti MD, Tagawa T, Miyata T. Ultra-long cycle fatigue of high-strength carbon steels part II: Estimation of fatigue limit for failure from internal inclusions. Mater Sci Eng A 2003;356:236–44. https://doi.org/10.1016/S0921-5093(03)00136-9.

[39] Yeşildal R. The effect of heat treatments on the fatigue strength of H13 hot work tool steel. Preprints 2018. https://doi.org/10.20944/preprints201812.0226.v1.

[40] Tridello A. VHCF response of two AISI H13 steels: Effect of manufacturing process and size-effect. Metals (Basel) 2019:9. https://doi.org/10.3390/met9020133.

[41] Pyttel B, Canteli AF, Ripoll AA. Comparison of different statistical models for description of fatigue including very high cycle fatigue. Int J Fatigue 2016;93:435–42. https://doi.org/10.1016/j.ijfatigue.2016.04.019.

[42] Tridello A, Paolino DS. LCF-HCF strain – life model : Statistical distribution and design curves based on the maximum likelihood principle 2023:2168–79. 10.1111/ffe.13990.

[43] Tridello A, Fiocchi J, Biffi CA, Chiandussi G, Rossetto M, Tuissi A, et al. Effect of microstructure, residual stresses and building orientation on the fatigue response up to 109 cycles of an SLM AlSi10Mg alloy. Int J Fatigue 2020;137:105659.